

High-Extinction-Ratio and Fabrication-Tolerant Polarization Beam Splitter based on Grating-Assisted Contradirectional Couplers

Yong Zhang, Yu He, Jiayang Wu, Ruili Liu, Ciyuan Qiu, and Yikai Su

State Key Lab of Advanced Optical Communication Systems and Networks, Department of Electronic Engineering, Shanghai Jiao Tong University, Shanghai 200240, China

Author e-mail address: yongzhang@sjtu.edu.cn

Abstract: A fabrication-tolerant polarization beam splitter (PBS) based on grating-assisted contradirectional couplers is experimentally demonstrated. Over 30-dB extinction ratios are achieved for both polarizations. Large fabrication tolerance in coupling length is also verified.

OCIS codes: (230.3120) Integrated Optics; (230.5440) Polarization-selective devices.

1. Introduction

Silicon nanowire waveguides with high index-contrast between silicon core and the cladding generally have considerable birefringence values, which result in polarization-dependent dispersions or losses for integrated devices [1]. Polarization beam splitters (PBSs) for splitting two orthogonal polarization modes are key components in polarization-diversity schemes to eliminate the polarization sensitivities [2]. A number of solutions were proposed to realize PBS devices, including multimode interference (MMI) structure [3], directional coupler (DC) [4], photonic crystal [5], hybrid plasmonic waveguide [6], out-of-plane grating [7], and so forth. Polarization extinction ratios (PERs) of previously reported PBSs were below 30 dB except one in [8], which was based on DC. However, optical coupling between the two waveguides in the DC-based PBS was periodically dependent on the coupling length and sensitive to fabrication variations. The PER of the DC-based PBS decreased from 20 dB to 12 dB when coupling length varied from $6.5 \mu\text{m}$ to $5.5 \mu\text{m}$ [9]. Recently, a compact PBS based on asymmetrical grating-assisted contradirectional couplers (GACCs) was theoretically proposed [10]. An advantage of such PBS is that it does not require stringent phase matching and coupling length. However, no experimental demonstration of such GACC-based PBS was reported.

In this paper, we experimentally demonstrate the first PBS based on GACCs. The device is fabricated on a silicon-on-insulator (SOI) wafer with a total length of $< 30 \mu\text{m}$. The coupling of TE mode between the two waveguides is strongly enhanced by GACCs, while the coupling of TM mode does not occur. Optical coupling between the two waveguides is monotonically dependent on the coupling length and insensitive to it. To realize single etch process and simple fabrication, symmetrical vertical structure is used in our design, which differs from that in [10]. The upper cladding of both waveguides is air. The PERs of the fabricated PBS are $> 30 \text{ dB}$ for both polarizations in a broad wavelength range ($\sim 20 \text{ nm}$). If coupling length varies from $27.52 \mu\text{m}$ to $20.64 \mu\text{m}$, the PERs still remain higher than 20 dB for both polarizations. To the best of our knowledge, our device achieves record high PERs with insensitive coupling length on silicon, enabling fabrication-tolerant mass production of the PBS devices.

2. Device design and fabrication

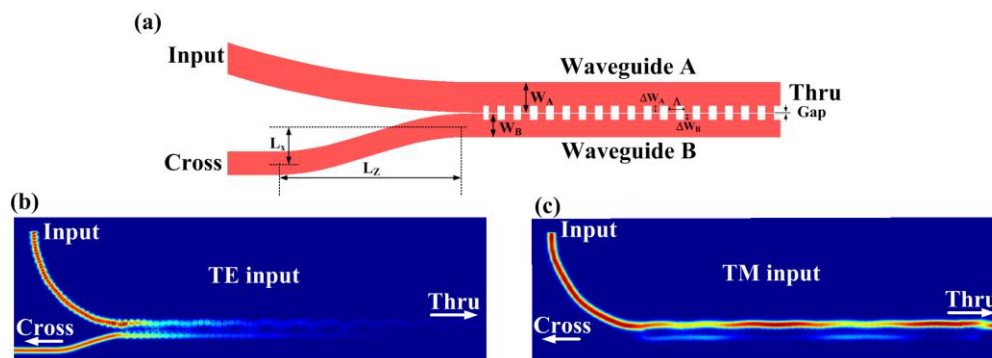


Fig. 1 (a) Schematic structure of the GACC-based PBS. (b)-(c) Simulated power distributions in the GACC-based PBS for TE-polarized and TM-polarized input, respectively.

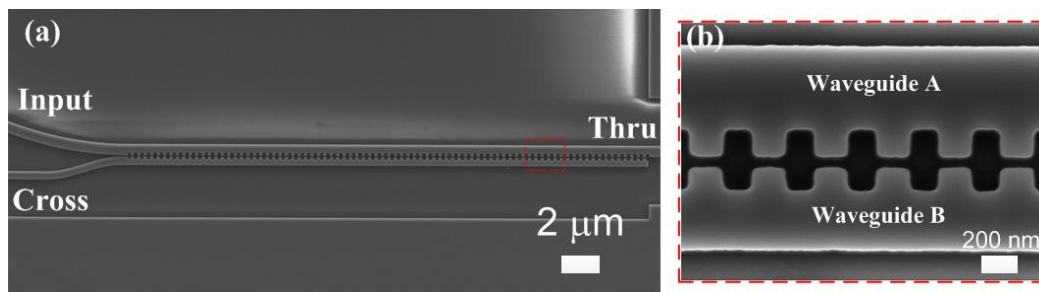


Fig. 2 (a) SEM image of the fabricated GACC-based PBS with corrugations period number $N = 80$. (b) Magnified micrograph of the GACC.

The GACC-based PBS is schematically illustrated in Fig. 1(a). The device consists of two parallel silicon strip waveguides, A and B. The bent waveguide and S-bend are at Input port and Cross port to make the two waveguides separated, respectively. The corrugations on the sidewall of the two waveguides are designed to form grating structures. The GACC is designed to enhance the coupling of TE mode, but has no effect on the coupling of TM mode. Therefore, TE-polarized light is contra-directionally coupled from waveguide A to waveguide B by the periodic corrugations. High power TE-polarized light is obtained in the Cross port. TM-polarized light goes through waveguide A without coupling. High power TM-polarized light is obtained in the Thru port. Thus, TE- and TM-polarized light are separated by the GACC. It is noted that, the asymmetrical configuration in on-plane direction can suppress the co-directional coupling between the waveguides. Symmetrical structure in normal direction is used in our design to realize single etch process and simple fabrication.

In the PBS structure, the thickness of silicon waveguides is 220 nm. The radius of bent waveguide at the Input port is 18 μm , which is large enough to ensure low-loss for TM-polarized light. The width of the waveguides are $W_A = 600$ nm and $W_B = 450$ nm, respectively. The period of the corrugation is $\Lambda = 344$ nm. The duty cycle of the corrugations is 52%. The corrugation widths are $\Delta W_A = 137$ nm and $\Delta W_B = 123$ nm, respectively. The gap between the waveguides is 65 nm. The offsets for the S-bend are $L_x = 0.8$ μm and $L_z = 4$ μm . The coupling length is determined by the period Λ and corrugation period number N . Three-dimensional finite-difference time-domain (3D-FDTD) method is applied to simulate the proposed structure ($N=60$). The radius of bent waveguide at the Input port is reduced to 5 μm to decrease simulation time in the simulation. The simulated power distributions for the TE- and TM- polarized light inputs are shown in Figs. 1(b) and (c), respectively. If a TE-polarized light is injected into the Input port, the light is contra-directionally coupled to the cross waveguide and outputs from the Cross port. While for a TM-polarized input, the light directly goes through waveguide A and outputs from the Thru port.

In the experiment, the GACC-based PBSs were fabricated on a SOI wafer (220-nm-thick silicon on 3000-nm-thick silica). E-beam lithography (Vistec EBPG 5200) was used to define the structures on the ZEP520A resist. Then the patterns were transferred to the top silicon layer by inductively coupled plasma (ICP) dry etching using SF_6 and C_4F_8 gases. Scanning electron microscope (SEM) images of the fabricated GACC-based PBS with corrugation period number $N=80$ are shown in Fig. 2.

3. Experiment results

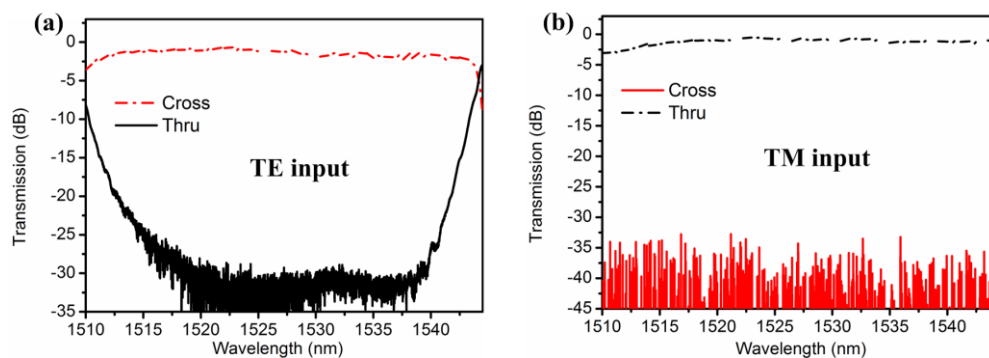


Fig. 3 Measured transmission responses at the Cross and Thru ports for (a) TE-polarization and (b) TM-polarization. The corrugation period number N and coupling length of the fabricated PBS are 80 and 27.52 μm , respectively.

In the measurements, TE- and TM- polarized lights from a tunable laser are coupled into/out of the chip by grating couplers, respectively. The grating couplers have significant polarization dependences. The coupling losses of the TE- and TM- polarized grating couplers are 7.7 dB/port and 8.7 dB/port at the grating central wavelengths,

respectively. Figures 3(a) and (b) show the measured transmission responses at the Cross and Thru ports of the fabricated PBS when TE- and TM- polarized lights are injected, respectively. The corrugation period number N is 80, and the coupling length is $27.52 \mu\text{m}$. Two identical PBSs are fabricated to measure responses for TE- and TM-polarized lights inputs, respectively. The responses are normalized by the transmission of a straight waveguide with grating couplers. For the TE-polarized light, the PER is higher than 30 dB in the wavelength range of $1517 \text{ nm} \sim 1538 \text{ nm}$, and the insertion loss is $< 1 \text{ dB}$. For the TM-polarized light, the PER is higher than 30 dB in the wavelength range of $1510 \text{ nm} \sim 1544 \text{ nm}$, and the insertion loss is $< 1 \text{ dB}$ from 1517 nm to 1544 nm . Some noise observed in Fig. 3 is attributed to that the received power is beyond the detection limit of the optical power meter.

In order to test the fabrication tolerance in coupling length, PBSs with different coupling lengths were fabricated. The measured responses for the fabricated PBSs with coupling lengths of $24.08 \mu\text{m}$ and $20.64 \mu\text{m}$ are shown in Figs. 4(a) and (b), respectively. In Fig. 4(a), for the TE-polarized light, the PER is higher than 20 dB in the wavelength range of $1513 \text{ nm} \sim 1530 \text{ nm}$, and the insertion loss is $< 2 \text{ dB}$. For the TM-polarized light, the PER is higher than 20 dB in the wavelength range of $1510 \text{ nm} \sim 1544 \text{ nm}$, and the insertion loss is $< 1.5 \text{ dB}$. In Fig. 4(b), for the fabricated PBS with a coupling length of $20.64 \mu\text{m}$, the PERs still remain higher than 20 dB for both polarizations in the wavelength range of $1515 \text{ nm} \sim 1537 \text{ nm}$, and the insertion losses are $< 1 \text{ dB}$. These results verify that the presented PBSs have a large fabrication tolerance in coupling length.

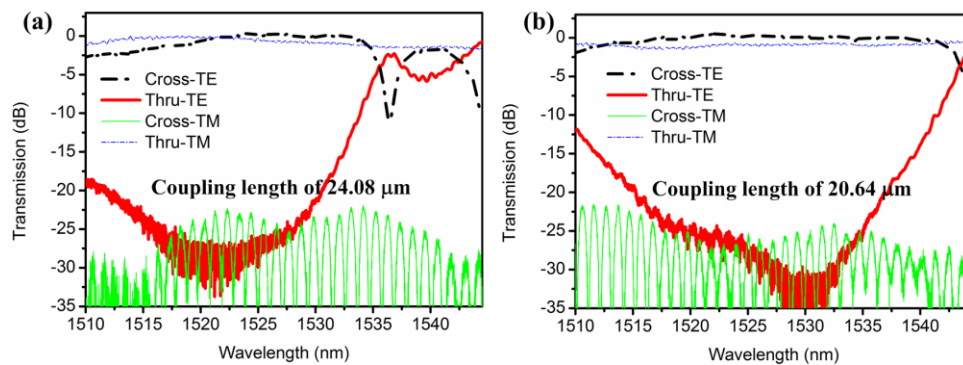


Fig. 4 Measured transmission responses at the Cross and Thru ports for TE- and TM- polarizations of the fabricated PBSs with (a) corrugation period number $N=70$, coupling length of $24.08 \mu\text{m}$, (b) corrugation period number $N=60$, coupling length of $20.64 \mu\text{m}$.

4. Conclusions

To the best of our knowledge, we have experimentally demonstrated a compact silicon PBS based on GACCs for the first time. The PBSs are realized by single etch process and simple fabrication. The PERs and insertion losses of the fabricated PBSs are $> 30 \text{ dB}$ and $< 1 \text{ dB}$, respectively, for both polarizations in a broad wavelength range of 20 nm. Due to the coupling enhanced by the GACCs, the coupling length does not need rigorous control. With the coupling length varied from $27.52 \mu\text{m}$ to $20.64 \mu\text{m}$, the PERs still remain $> 20 \text{ dB}$ and the insertion losses are $< 2 \text{ dB}$ for both polarizations. These results show that the PBSs have a large fabrication tolerance in coupling length.

References

1. C. Manolatu, and H. A. Haus, "High density integrated optics," in *Passive Components for Dense Optical Integration*(Springer, 2002), pp. 97-125.
2. B. Shen, P. Wang, R. Polson, and R. Menon, "An integrated-nanophotonics polarization beamsplitter with $2.4 \times 2.4 \mu\text{m}^2$ footprint," *Nature Photonics* **9**, 378-382 (2015).
3. B. Rahman, N. Somasiri, C. Themistos, and K. Grattan, "Design of optical polarization splitters in a single-section deeply etched MMI waveguide," *Applied Physics B* **73**, 613-618 (2001).
4. J. Wang, D. Liang, Y. Tang, D. Dai, and J. E. Bowers, "Realization of an ultra-short silicon polarization beam splitter with an asymmetrical bent directional coupler," *Optics Letters* **38**, 4-6 (2013).
5. X. Ao, L. Liu, L. Wosinski, and S. He, "Polarization beam splitter based on a two-dimensional photonic crystal of pillar type," *Applied Physics Letters* **89**, 171115 (2006).
6. Z. Su, E. Timurdogan, E. S. Hosseini, J. Sun, G. Leake, D. D. Coolbaugh, and M. R. Watts, "Four-port integrated polarizing beam splitter," *Optics Letters* **39**, 965-968 (2014).
7. J. Feng, and Z. Zhou, "Polarization beam splitter using a binary blazed grating coupler," *Optics Letters* **32**, 1662-1664 (2007).
8. A. Xie, L. Zhou, J. Chen, and X. Li, "Efficient silicon polarization rotator based on mode-hybridization in a double-stair waveguide," *Optics Express* **23**, 3960-3970 (2015).
9. D. W. Kim, M. H. Lee, Y. Kim, and K. H. Kim, "Planar-type polarization beam splitter based on a bridged silicon waveguide coupler," *Optics Express* **23**, 998-1004 (2015).
10. H. Qiu, Y. Su, P. Yu, T. Hu, J. Yang, and X. Jiang, "Compact polarization splitter based on silicon grating-assisted couplers," *Optics Letters* **40**, 1885-1887 (2015).